On-treatment dynamics of circulating extracellular vesicles (EVs) in the first-line setting of patients with advanced non-small cell lung cancer (NSCLC): the LEXOVE prospective study

VALERIO GRISTINA
University Hospital Policlinic Paolo Giaccone: Azienda Ospedaliera Universitaria Policlinico
Viviana Bazan
University Hospital Policlinic Paolo Giaccone: Azienda Ospedaliera Universitaria Policlinico
Nadia Barraco
University Hospital Policlinic Paolo Giaccone: Azienda Ospedaliera Universitaria Policlinico
Simona Taverna
National Research Council: Consiglio Nazionale delle Ricerche
Mauro Manno
National Research Council: Consiglio Nazionale delle Ricerche
Samuele Raccosta
National Research Council: Consiglio Nazionale delle Ricerche
Marco Bono
University Hospital Policlinic Paolo Giaccone: Azienda Ospedaliera Universitaria Policlinico
Tancredi Didier Bazan Russo
University Hospital Policlinic Paolo Giaccone: Azienda Ospedaliera Universitaria Policlinico
Francesco Pepe
University of Naples Federico II: Universita degli Studi di Napoli Federico II
Pasquale Pisapia
University of Naples Federico II: Universita degli Studi di Napoli Federico II
Lorena Incorvaia
University Hospital Policlinic Paolo Giaccone: Azienda Ospedaliera Universitaria Policlinico
Giuseppe Badalamenti
University Hospital Policlinic Paolo Giaccone: Azienda Ospedaliera Universitaria Policlinico
Giancarlo Troncone
University of Naples Federico II: Universita degli Studi di Napoli Federico II
Umberto Malapelle
University of Naples Federico II: Universita degli Studi di Napoli Federico II
Daniele Santini
University of Rome La Sapienza: Universita degli Studi di Roma La Sapienza

Antonio Russo (antonio.russo@usa.net)
University Hospital Policlinic Paolo Giaccone: Azienda Ospedaliera Universitaria Policlinico
Antonio Galvano
University Hospital Policlinic Paolo Giaccone: Azienda Ospedaliera Universitaria Policlinico

---

Research Article

Keywords: NSCLC, liquid biopsy, EVs, DLS, dynamics

Posted Date: December 19th, 2023

DOI: https://doi.org/10.21203/rs.3.rs-3757085/v1

Abstract

Introduction:

The evaluation of extracellular vesicles (EVs) might be a complementary tool to assess response in the clinic. We aimed to describe whether the serial characterization of EVs could longitudinally reflect response and resistance to first-line treatments in advanced NSCLC.

Methods

Treatment-naïve patients with advanced NSCLC receiving osimertinib (osi), alectinib, pembrolizumab (pembro), or platinum-based chemotherapy (CT) ± pembro were prospectively enrolled at the University Hospital of Palermo, Italy. Isolated EVs were characterized by Static and Dynamic Light Scattering (DLS) to assess the size distribution and amount of vesicles (R90, Dz and PDI). EV protein amount was evaluated by Bradford assay (BA) through the quantification of circulating cell-free EV protein content (cfEV). According to the radiologic response, cfEV and R90 kinetics were evaluated in patients from baseline (T0) to the first radiologic restaging (T1) with a 20% cfEV increase being used as the cut-off point for median progression-free survival (mPFS) analysis.

Results

Among 27 consecutive patients, a total of 135 plasma samples were collected both at T0 and T1 to isolate EVs. Purified EVs were characterized by WB for ALIX and TSG-101. EV size was determined by DLS showing an average size ranging from 183 to 260 nm. The mean cfEV value at T0 and at T1 time was 1.26 and 1.49 µg/ml, respectively ($p = 0.02$). Within the cfEV responsive group, 13 patients had a clinically improved mPFS (25.2 months, 95% CI: 14.9–35.5) when compared to 11 cfEV non-responders (8.3 months, 95% CI: 3.6–12.9) ($p = 0.07$). Namely, cfEV responders receiving single-agent pembro experienced a significantly improved mPFS (25.2 months, 95% CI: 11.7–38.8; $p = 0.04$) compared to patients receiving CT plus pembro (6.1 months, 95% CI: 1.1–11.1; $p = 0.9$). EGFR-positive cfEV responders showed a clinically improved mPFS (35.1 months, 95% CI: 14.9–35.5) as compared to cfEV non-responders (20.8 months, 95% CI: 11.2–30.4) ($p = 0.06$). In the EGFR-mutated subgroup, four patients with R90 decreasing values are still responding whereas one patient with R90 increasing value had a rapidly progressive disease.

Conclusions

This study showcased the feasibility of the serial on-treatment monitoring of plasma EVs in the first-line setting of NSCLC, mostly in those patients receiving single-agent pembro or osi. The increased amount of

circulating EVs (R90) and the higher level of associated proteins (cfEV) warrant larger controlled studies to explore EVs as novel promising liquid biopsy biomarkers.

Introduction

Despite the increasing availability of diagnosis and personalized therapeutic approaches, most patients with non-small cell lung cancer (NSCLC) usually present with an advanced stage of disease, regrettably showing very low 5-year survival rates [1]. Although several biomarkers have been described in this complex scenario [2] [3] [4], there remains an unmet clinical need for the discovery of dynamic *in vivo* biomarkers to refine the clinical management of such patients, predicting response and prognostics to eventually improve the treatment sequencing while avoiding ineffective therapies.

Over the last decade, emphasis has been placed on nano/micrometer-sized vesicles for their role in intercellular communications contributing to tumor growth, metastasis, angiogenesis, and drug resistance [5]. Extracellular vesicles (EVs) are a heterogeneous group of double membrane-enclosed vesicles released by all cytotypes in physiological and pathological conditions [6]. EVs are classified based on their size, origin, and release mechanism [7]–[10], shuttling a plethora of bioactive molecules such as proteins, lipids, metabolites, and nucleic acids [11]–[13].

In the liquid biopsy era, albeit the circulating cell-free DNA (cfDNA) analysis remains the gold standard for routine clinical diagnostics [14], the evaluation of EV amount and morphology might be a complementary tool to assess response and guide the clinical decision-making process [15]. Accordingly, a growing body of evidence has proved the utility of circulating EVs as minimally invasive biomarkers in different disease settings, even if often at the preclinical level [16]–[17]. Compelling evidence suggests that the anti-tumor response is a multifaceted process regulated by intricate interactions among the tumor, the immune system, and various host factors in which EVs seem to hold a pivotal role [18][19]. Therefore, clinical cohort trials in real-life settings are needed to evaluate if serial sampling of tumor-derived plasma EVs may enable on-treatment monitoring of patients with advanced NSCLC.

From this perspective, differing methods of EV isolation and characterization have been set out with Dynamic Light Scattering (DLS) representing a promising technique for determining the particle size distribution in a colloidal suspension such as human plasma [20]. Making use of the brownian motion of suspended particles in a solvent, DLS would enable the analysis of nanoparticles by evaluating the hydrodynamic diameter (Dz) and the Rayleigh scattering (R90) to compare the concentration of equally sized and shaped nanoparticles [21]. Furthermore, the quantification and dynamics of EV biophysical properties and total protein content during first-line systemic treatments have never been prospectively evaluated as a potential clinical tool in NSCLC.

In this explorative study, we aimed to describe whether the serial characterization of plasma tumor-derived EVs could longitudinally reflect response and resistance to available first-line treatments, investigating the potential to predict clinical outcomes in patients with advanced NSCLC.

Materials and methods

Study design and patients

The Lung EXtracellular VEsicles (LEXOVE) study is a prospective cohort observational trial aiming to investigate circulating EVs as potential and minimally invasive biomarkers for monitoring and prognostics of treatment-naïve patients with advanced NSCLC undergoing standard first-line treatments (Fig. 1). From February 2020 to May 2022, patients with advanced NSCLC treated at the Medical Oncology Unit of Paolo Giaccone University Hospital of Palermo, Italy, were consecutively enrolled. FFPE tissue collection, nucleic acid extraction, and molecular analysis are comprehensively described in the Supplementary methods. Paired blood samples were collected at baseline (T0) and the first radiologic evaluation of disease within 12 ± 1 weeks (T1 or W12) during the treatment course. The collected plasma samples were used to isolate EVs that were characterized by either DLS or Bradford assay (BA). All the patients underwent a computerized tomography scan every 3 months and radiologic responses were classified according to the Response Evaluation Criteria in Solid Tumors (RECIST) version 1.1. Clinical and pathological characteristics of all patients included in our study were retrieved from the clinical records available. Inclusion criteria considered: (1) Eastern Cooperative Oncology Group (ECOG) Performance Status (PS) of ≤ 2; (2) patients with histologically- or cytologically-documented NSCLC with unresectable stage IIIB-C or Stage IV Disease (according to Version 8 of IASLC TNM) who were treatment-naïve and eligible for first-line active systemic treatment according to clinical practice (osimertinib [osi], alectinib, pembrolizumab [pembro] or platinum chemotherapy [CT]-based treatments [CT +/- pembro]). Exclusion criteria included: (1) patients with other malignant tumors; (2) patients with ECOG PS ≥ 3; (3) patients who received prior systemic oncological treatment; (3) patients with mental illness prohibiting informed consent. Of note, to reduce the interference with EVs isolation and kinetics, only patients not affected by other medical conditions and not receiving other concomitant medications were finally considered for study analysis. The study was conducted following the Declaration of Helsinki, and the protocol was approved by The Ethics Committee Palermo I (AIFA code CE 150109).

Blood samples and plasma separation

Blood samples (5 mL) were collected into K_2 EDTA tubes (BD Vacutainer®) early in the morning with fasting required. Blood samples from included patients were collected at baseline before the first drug administration and at each instrumental disease re-evaluation during the treatment course according to clinical practice. Blood samples from healthy controls were collected at baseline and after twelve weeks of follow-up, and treated equally. As previously described [22], blood specimens were immediately processed for plasma collection and centrifuged twice. The first refrigerated centrifugation was performed using low force for 10 minutes at 1.200 x *g* to retain the vast majority of EVs and exclude cellular material. The second centrifugation was carried out for 10 minutes at 16.000 x *g* to completely remove some of the large vesicles including cellular fragments and cell debris. Sample processing was carried out within 15 minutes of blood collection. An aliquot (2ml) of collected plasma from both patients

and healthy controls was immediately processed for isolating EVs, whereas other aliquots were frozen at -80°C for subsequent biophysical or biological analysis. Further, to remove the cryoprecipitates, the appropriately thawed plasma aliquot was centrifugated for 5 minutes at 3.000 x g and 4°C before the EV isolation steps.

Extracellular vesicles isolation

According to the most recent ISEV guidelines [23], following serial centrifugation steps, EVs were isolated using a membrane affinity-based method [24] [9]. Briefly, EVs were isolated using the exoEasy Maxi Kit (Qiagen, Hilden, Germany), based on a membrane affinity purification method, according to the manufacturer's protocol. Specifically, non-vesicular proteins along with organic polymers and other impurities were washed out during a column-based centrifugation procedure using such a membrane affinity method. Healthy control samples were treated equally.

Extracellular vesicles characterization by Western Blot (WB)

EVs were analyzed to detect specific proteins well-known as markers of the EV population. 20 µg of EVs were resolved by Novex Bis-Tris SDS-acrylamide gels (Invitrogen, Life Technologies, USA) in reducing conditions and with heating. After the electrophoresis, proteins were transferred to nitrocellulose membranes (GE Healthcare Life Sciences, Boston, USA) and non-specific binding sites were blocked by incubating membranes in a blocking solution: 10% non-fat dry milk (Sigma-Aldrich, St Luis, USA) in Tris-Buffer Saline, 0.1% Tween (TBS-T), for 60 min, at room temperature. Then, membranes were incubated overnight at 4°C with monoclonal anti-TSG-101 (dilution 1:500; sc-7964) and ALIX (dilution 1:500; sc-53540) antibodies; after three washes in TBS-T, the membranes were incubated with specific secondary HRP-antibodies (dilution 1:10000) for 1 hour (Santa Cruz, Biotechnology Inc). Chemiluminescence was detected using Chemidoc system (BioRad ,Hercules, California, USA).

Extracellular vesicles quantification by Bradford assay (BA)

EV-protein levels defined as cell-free EV protein content (cfEV) were determined using BA. In brief, 10 µl of EVs resuspended in PBS were added to 200 µl of Coomassie Protein Assay Reagent (Pierce, Rockford, IL, USA). The absorbance at 595 nm was measured using the spectrophotometer (SPECTROstar nano BMG LABtech). The protein concentration was calculated using a standard curve of a dilution series of bovine serum albumin (BSA, Merck, Darmstadt, Germany) according to standard protocols from our group [25].

Extracellular vesicles characterization by Dynamic Light Scattering (DLS)

DLS assay was used to evaluate the biophysical biomarker of an aliquot of isolated EVs from patients and healthy subjects using PBS and a commercial elution buffer (XE, Qiagen) as negative controls. Each isolated EV sample was poured directly into a quartz cuvette and centrifugated at 1.000 x *g* for 10 minutes and 4°C to remove any dust particles. Subsequently, isolated EVs were placed at 20°C in a thermostatic cell compartment of a BI200-SM goniometer (Brookhaven Instruments) equipped with a He-Ne laser (JDS Uniphase 1136P) at 633 nm and a single pixel photon counting module (Hamamatsu

C11202-050). The scattered light intensity and its time autocorrelation function g2(t) were measured simultaneously at 90° by using a BI-9000 correlator (Brookhaven Instruments). Absolute values for scattered intensity (excess Rayleigh ratio at 90°, R90) were obtained by normalization to toluene and subtraction of the buffer signal [26]. R90 is proportional to the particle number concentration N, the squared weight-averaged mass (Mw)2, and the form factor P(q); therefore, in the case of particles with the same size and shape, it can be considered as a rough esteem of the vesicle amount [27]. The autocorrelation functions were fitted by a two-component Schultz distribution for the diffusion coefficient D [28][29]. Then, the intensity-weighted distribution of hydrodynamic radii Dh is determined by using the Stokes-Einstein relation $D = (kBT)/(3\pi\eta Dh)$, where kB is the Boltzmann constant, T is the temperature, and η is the medium viscosity, that is assumed to be the same as PBS. Indeed, a DLS measurement was performed both on a vesicle sample in buffer XE and the same sample in PBS. This buffer exchange was performed by HPLC-SEC run on a Sepharose CL-2B column by recovering the void volume fraction to eliminate the small-sized particles due to buffer XE. The first component of the distribution (not shown) amounts to less than 5% of the signal and refers to small-size particles (less than 20 nm) present in the samples. By considering the second component of the distribution, which is related to vesicles, one measures the average and the normalized variance, corresponding to the z-averaged hydrodynamic diameter (Dz) and the polydispersity index (PDI) of vesicle distribution, respectively [30].

Statistical considerations

Descriptive statistics were used to analyze demographic and clinical data. According to radiologic response, efficacy was defined as responsive (complete response [CR] or partial response [PR]) or non-responsive disease (stable disease [SD] or progressive disease [PD]), based on the standard RECIST 1.1 criteria. A paired Wilcoxon test was used to compare the mean EV plasma levels before and after the treatment course. Regarding cfEV, we dichotomized values as $\geq$ and < 20% indicating the change from baseline cfEV to higher and lower levels, respectively, after the initiation of treatment. The Kaplan–Meier method was used to perform survival analysis providing median values and their 95% confidence interval (CI) with p-values, while the log-rank test was selected for comparisons. Univariable and multivariable analyses were performed using the Cox proportional hazards regression models. The multivariable model included as covariates all pretreatment clinically meaningful parameters and/or statistically significant p-values at univariable analysis. A logistic regression model was performed to evaluate the relationship between one or more independent variables with a dependent one. Progression-free survival (PFS) was calculated from the date of study inclusion to the first evidence of disease progression or death from any cause or censored at the most recent follow-up. A p-value < 0.05 was used as the threshold for statistical significance. All the statistical analyses were performed using SPSS statistics software, version 20 (IBM, Armonk, NY, USA).

Results

With a median follow-up of 34.2 months (range: 24.8–42.0 months), among 87 patients meeting the eligibility criteria, 27 consecutive patients with advanced NSCLC and no other medical conditions or

concomitant medications were prospectively included. Briefly, a total of 135 liquid biopsy samples were collected isolating EVs from 27 patients at baseline with paired available plasma samples at disease radiologic re-evaluation. To discover and validate any EV-based biomarkers in the advanced setting of NSCLC, we further categorized the overall population by specific treatment subgroups including 8, 6, and 9 patients receiving osi, pembro, and CT +/- pembro, respectively. Clinicopathological characteristics are summarized in Supplementary Table S1. In addition, BA and DLS analyses were performed on two healthy volunteers (one female and one male) to highlight any significant differences between patients with NSCLC and healthy controls.

Plasma EVs characterization and frequencies over treatment

Specific markers, protein content, size, and amount of plasma-EVs were examined to demonstrate their nature and purity (Fig. 2). Isolated EVs were characterized via WB revealing conventional EV markers such as Aand TSG-101. Four representative samples (one for each specific treatment subgroup) are shown in Fig. 2C. Morphological analysis of EVs was performed by DLS taking into consideration R90, Dz, and PDI values. DLS showed a Dz value ranging from 183 to 260 nm with an average size of 228.5 and 233.7 nm at baseline and restaging, respectively, without any on-treatment significant differences in diameters ($p = 0.24$) (Fig. 3, Supplementary Table S2). An average R90 value of 2964.75 and 2315.54 $10 - 6$ cm-1 was found at time T0 and T1 with no significant changes regarding the amount of EVs over therapy ($p = 0.21$) (Fig. 3, Supplementary Table S2). We observed an average PDI value of 0.21 and 0.18 at baseline and restaging, showing statistically significant differences in the width of distribution size of EVs over treatment ($p = 0.03$) (Fig. 3, Supplementary Table S2). BA of plasma EVs showed a mean protein value of purified cfEVs of 1.26 and 1.49 µg/ml at baseline and restaging, respectively, resulting in statistically significant changes during the treatment course ($p = 0.02$) (Fig. 3, Supplementary Table S2).

Compared to healthy donors, treatment-naïve patients with advanced NSCLC presented with higher levels of both EV protein content and total vesicles along with steadily higher cfEV and R90 values both at baseline and following systemic treatment (Supplementary Table S2). Interestingly, DLS analyses revealed smaller size and less dispersed distribution for EVs isolated from treatment-naïve patients with NSCLC (Fig. 4, Supplementary Table S2).

Association of plasma EVs dynamics with survival according to treatment subgroups

As previously evaluated for cfDNA kinetics [22], we evaluated the dynamics of cfEV in the overall cohort population and across treatment subgroups according to available plasma samples, detecting a 20% median increase of cfEV as the cut-off point for analyses of patients receiving osi, pembro or CT +/- pembro. Overall, 13 patients with Δ cfEV decrease had clinically improved mPFS (25.2 months, 95% CI: 14.9–35.5) when compared to 11 patients with Δ cfEV increase (8.3 months, 95% CI: 3.6–12.9), trending to the formal significance ($p = 0.07$) (Fig. 5). Namely, dealing with treatment subgroups, patients receiving

single-agent pembro with decreasing Δ cfEV levels presented with a statistically improved mPFS (25.2 months, 95% CI: 11.7–38.8) compared to those patients with increasing Δ cfEV (6.8 months, 95% CI: 0-6.8) (p = 0.04). To the contrary, no differences in mPFS according to Δ cfEV were observed in the CT +/- pembro group (6.1 [95% CI: 1.1–11.1] vs 8.3 months [95% CI: 7.7–10.1]; p = 0.9). Intriguingly, EGFR-positive patients receiving osi with Δ cfEV decrease tended to experience longer mPFS (35.1 months, 95% CI: 14.9–35.5) as compared to patients with increasing Δ cfEV values (20.8 months, 95% CI: 11.2–30.4) (p = 0.06). Interestingly, four patients with R90 decreasing values are still responding whereas one patient with R90 increasing valuehad a rapidly progressive disease. Figure 6 depicts the Kaplan–Meier plot of PFS according to treatment subgroups in patients Δ cfEV decrease.

Univariable and multivariable associations between potential risk factors and extracellular vesicles dynamics

Different clinical variables were evaluated as potential independent risk factors for PFS or cfEV dynamics using Cox proportional hazards regression analysis. The tested variables were gender, age, smoking status, histology, treatment, tissue PD-L1 expression levels, and cfEV kinetics. Finally, the multivariable analyses suggested ECOG PS of 2 as the only independent risk factor for survival whereas none of the tested clinical parameters resulted in significantly affecting the cfEV dynamics during the treatment course (Supplementary Tables S3-S4).

Longitudinal monitoring by liquid biopsy data

Finally, focusing on patients with sufficient biospecimens for EV analysis and at least two clinical follow-ups for therapeutic assessment, here we report the graphical representation of the results of the longitudinal monitoring by liquid biopsy (cfEV and R90) (Figure 7).

Discussion

Despite emerging personalized treatments have dramatically changed the clinical practice of NSCLC, unfortunately, the prognosis of such patients with advanced disease remains poor with treatment response being regrettably confined to specific subsets of patients [31]. In the precision oncology era, research on biomarker-driven treatment has been rapidly evolving with different liquid biopsy analytes being intensively investigated for diagnosis and prognostication in the most common solid tumors [14]. Over the last decade, a growing body of emerging preclinical data supported the investigation of EVs as a compelling source of cancer biomarkers leading to differing retrospective series that evaluated the sampling of plasma EVs as a promising approach to dynamically track the real-time cancer behavior [32] [33]. However, the significance of EV contents in *ex-vivo* samples from prospective clinical cohort trials remains poorly understood. In this fascinating scenario, we designed a prospective biomarker trial to evaluate the dynamics of plasma EVs profile as prognostic and/or predictive biomarkers in the first-line clinical setting of NSCLC.

First, we demonstrated the feasibility of isolating and accurately characterizing EVs from the plasma of treatment-naïve patients in a real-life setting of advanced NSCLC. To improve the separation efficiency and enrichment during the isolation steps, we used serial centrifugation steps followed by a membrane affinity-based method that could yield purified vesicle fraction by largely removing co-isolating structures (such as protein complexes or lipoproteins, especially abundant in plasma), thus confirming the improved performance of combined isolation methods when dealing with clinical samples [34] [35]. EV characterization, through the evaluation of well-known protein markers, was assessed by WB. EV protein amount was evaluated by BA, an informative, cheap, and easy-to-use colorimetric assay, that quantified the amount of EV protein content in our cohort. EV size was analyzed by integrating DLS, a brownian motion-based technique that evaluated the integrity and purity of EVs, taking into consideration R90, Dz and PDI for the estimation of the number, diameter, and size distribution of EVs, respectively. Overall, according to R90 and cfEV parameters, we noted that the number of EVs and their protein levels were significantly increased in the plasma of NSCLC patients compared to healthy donors. This was consistent with previous reports that however used dissimilar techniques such as transmission electron microscopy and flow cytometry [36]. As reflected by Dz values, we reported a smaller size for EVs isolated from NSCLC patients compared to healthy subjects. Finally, considering a PDI value not greater than 0.4 in both healthy and cancer individuals, we detected a homogenous population of vesicles within monodispersed plasma samples [37]. Noteworthy, it should be considered that the biological response of EV cargo could be affected by its dispersion state and solubility in plasma. In our study, compared to microscopy techniques, DLS provided additional data of paramount significance on the biodistribution of nanoparticle properties. An added advantage is that DLS is not time-consuming, not as technically challenging, and does not result in any sample loss, making it a valuable and complementary approach for the quantification of plasma EV protein levels and the detection of residual small size co-isolates, especially when dealing with scant and precious patients' plasma samples [38]. These data support the use of DLS as a valid technique for characterizing *in vivo* EVs with a low limit of detection from the plasma of patients with advanced NSCLC, confirming previous findings from other solid tumors [39][40]. In addition, we leveraged the combination of DLS with BA to improve sample characterization and further investigate EV protein content, demonstrating that this approach in NSCLC patients allowed a quantitative and high-throughput characterization of purified EVs even in cases of limited sample volume.

Then, we asked whether the dynamics of plasma EVs from baseline to first radiologic re-staging could unveil patients' survival according to specific treatment subgroups. We observed that the level of plasma EV proteins and the width of EV distribution were significantly affected over time by the treatment course whereas EV amount and diameters did not show any statistically significant on-treatment variations. Interestingly, in the overall cohort, we observed that dynamic EV protein changes were associated with sustained treatment responses and clinically improved survival since responders exhibited decreasing levels of cfEV compared to a significant increase in non-responders. Strikingly, this was clinically prominent in those patients receiving pembro or osi, compared to those patients undergoing chemotherapy +/- pembro. In the pembro subgroup, the Δ cfEV was significantly associated with survival

(p=0.04) whereas in the osi arm the threshold for statistical significance was not formally reached (p=0.06). Importantly, we proved that cfEV kinetics was not affected by any baseline patients' clinical characteristics while, in line with other evidence, the multivariable analysis identified only ECOG PS as a potentially interfering risk factor associated with worse survival in the overall cohort [41].

The limitations of this study include the non-randomized design, the small sample size, the heterogeneity of clinical-pathological characteristics, and the lack of results in terms of overall survival. As regards the limited sample size, it should be noted that, to strictly limit any selection or sample analysis biases affecting the outcome of EV experiments, according to the latest ISEV guidelines we only considered and tested fasting plasma from a real-life consecutive series of advanced NSCLC patients presenting with no other co-existing medical conditions or concomitant medications [23]. Moreover, to test for the variability of EV-based features and to further validate our results, we analyzed matched intraindividual plasma samples with repeated plasma samples serving as controls not eventually affected by individual differences. Considering the immature follow-up and the absence of enough death events, here we did not present any results of EV dynamics in terms of overall survival that would however have been affected by subsequent treatment lines. Besides, a significant constraint could regard the use of DLS that could not characterize the specific phenotype of the isolated EVs, albeit resulting to be extremely useful when characterizing precious plasma samples. Nevertheless, this proof-of-concept study provided preliminary evidence on the potential role of plasma EVs as circulating biomarkers generating a study hypothesis that should be adequately addressed by larger prospective trials for obtaining accurate, reliable, and fast biomarkers of treatment response, mostly in those patients who are candidates to receive first-line single-agent pembro or osi.

Conclusions

The results of this study showcased the feasibility of the serial on-treatment monitoring of plasma EVs in the first-line setting of NSCLC, providing an added value in the real-time monitoring of treatment response which is more prominent in those patients receiving first-line single-agent pembro or osi. Besides the efficacy of the isolation methods and the purity of the retrieved EV fraction, some practical considerations such as costs, hands-on time, and the total duration of isolating procedures should be pondered [42]. The increased amount of circulating EVs (R90) and the higher level of associated proteins (cfEV), when compared to healthy subjects, might better reflect the biology of NSCLC. This evidence, together with the increased stability in plasma, warrants larger controlled studies to explore EVs as novel promising liquid biopsy biomarkers even for early cancer detection, as recently outlined [43]. Despite contemporary EV research extensively relies on a wide range of biochemical and physical analysis methodologies, it is essential to delve deeper into *in vivo* samples and validate such differing EV-based approaches in the clinic for diagnostic and therapeutic purposes.

Declarations

Conflict of Interest

The authors declare that the research was conducted in the absence of any commercial or financial relationships that could be construed as a potential conflict of interest.

Consent for publication

All the authors agree to the content of the paper and are listed as co-authors of the paper.

Author Contributions

Conceptualization: V.G., V.B., N.B.; methodology: V.G., N.B., S.T.; software: V.G., A.G.; validation: V.G., V.B., N.B., U.M., D.S.; formal analysis: V.G., N.B., M.M., S.R., A.G.; investigation: V.G., N.B., S.T., A.G., M.M., S.R; resources: V.G., N.B., V.B., S.T., S.R., M.M., A.R.; data curation: M.B., TD.BR., F.P., P.P., G.T.; writing—original draft preparation: V.G., N.B., M.M., S.R., A.G.; writing—review and editing: L.I., G.B., V.B., G.T., U.M., A.R., D.S.; visualization: V.G., N.B., S.T.; supervision: L.I., G.B., G.T., V.B., U.M., A.R., D.S., A.G.; project administration: V.G., N.B., V.B., A.R, D.S. All authors have read and agreed to the published version of the manuscript.

Funding

The authors have not declared a specific grant for this research from any funding agency in the public, commercial, or not-for-profit sectors.

Institutional Review Board Statement

The study was conducted according to the guidelines of the Declaration of Helsinki and approved by Palermo 1 Institutional Ethic Review Board (Statement No. 02/2020, approved on 19 February 2020, AIFA code CE 150109). Informed consent was obtained from all subjects involved in the study.

Acknowledgments

V.G. and TD.BR. contributed to the current work under the Doctoral Programme in Experimental Oncology and Surgery, University of Palermo.

Data Availability Statement

Data could be available upon reasonable request to the authors.

References

1. Siegel RL, Miller KD, Wagle NS, Jemal A. Cancer statistics, 2023. CA Cancer J Clin, 2023.
2. Galvano A et al. The prognostic impact of tumor mutational burden (TMB) in the first-line management of advanced non-oncogene addicted non-small-cell lung cancer (NSCLC): a systematic review and meta-analysis of randomized controlled trials. ESMO Open. 2021.

3. Gristina V, La Mantia M, Iacono F, Galvano A, Russo A, Bazan V. The emerging therapeutic landscape of alk inhibitors in non-small cell lung cancer. Pharmaceuticals. 2020.
4. Galvano A et al. Analysis of systemic inflammatory biomarkers in neuroendocrine carcinomas of the lung: prognostic and predictive significance of NLR, LDH, ALI, and LIPI score. Ther Adv Med Oncol, 2020.
5. Xavier CPR, Caires HR, Barbosa MAG, Bergantim R, Guimarães JE, Vasconcelos MH. The Role of Extracellular Vesicles in the Hallmarks of Cancer and Drug Resistance. Cells. 2020.
6. Möller A, Lobb RJ. The evolving translational potential of small extracellular vesicles in cancer., Nat. Rev. Cancer, vol. 20, no. 12, pp. 697–709, Dec. 2020.
7. Monteleone F, Taverna S, Alessandro R, Fontana S. SWATH-MS based quantitative proteomics analysis reveals that curcumin alters the metabolic enzyme profile of CML cells by affecting the activity of miR-22/IPO7/HIF-1alpha axis. J Exp Clin Cancer Res. Jul. 2018;37(1):170.
8. Candela ME, Geraci F, Turturici G, Taverna S, Albanese I, Sconzo G. Membrane vesicles containing matrix metalloproteinase-9 and fibroblast growth factor-2 are released into the extracellular space from mouse mesoangioblast stem cells., J. Cell. Physiol., vol. 224, no. 1, pp. 144–151, Jul. 2010.
9. Reclusa P et al. Improving extracellular vesicles visualization: From static to motion. Sci Rep, 2020.
10. Cocozza F, Grisard E, Martin-Jaular L, Mathieu M, Théry C. SnapShot: Extracellular Vesicles., Cell, vol. 182, no. 1, pp. 262–262.e1, Jul. 2020.
11. Galvano A, et al. Detection of RAS mutations in circulating tumor DNA: a new weapon in an old war against colorectal cancer. A systematic review of literature and meta-analysis. Ther Adv Med Oncol. 2019;11:1758835919874653.
12. Taverna S, Giusti I, D'Ascenzo S, Pizzorno L, Dolo V. May, Breast Cancer Derived Extracellular Vesicles in Bone Metastasis Induction and Their Clinical Implications as Biomarkers. Int J Mol Sci, vol. 21, no. 10, 2020.
13. Cammarata G, et al. Emerging noncoding RNAs contained in extracellular vesicles: rising stars as biomarkers in lung cancer liquid biopsy. Ther Adv Med Oncol. 2022;14:17588359221131228.
14. Russo A et al. The molecular profiling of solid tumors by liquid biopsy: a position paper of the AIOM–SIAPEC-IAP–SIBioC–SIC–SIF Italian Scientific Societies. ESMO Open. 2021.
15. García-Pardo M, Makarem M, Li JJN, Kelly D, Leighl NB. Integrating circulating-free DNA (cfDNA) analysis into clinical practice: opportunities and challenges. Br J Cancer. 2022.
16. Silva J et al. Analysis of exosome release and its prognostic value in human colorectal cancer. Genes Chromosom Cancer, 2012.
17. Li P, Qin C. Elevated circulating VE-cadherin + CD144 + endothelial microparticles in ischemic cerebrovascular disease. Thromb Res, 2015.
18. Lipinski S, Tiemann K. Extracellular vesicles and their role in the spatial and temporal expansion of tumor–immune interactions. Int J Mol Sci. 2021.

19. Yim KHW, Al Hrout A, Borgoni S, Chahwan R. Extracellular vesicles orchestrate immune and tumor interaction networks. Cancers. 2020.
20. Liu C, Yang Y, Wu Y. Recent Advances in Exosomal Protein Detection Via Liquid Biopsy Biosensors for Cancer Screening, Diagnosis, and Prognosis. AAPS J. 2018.
21. Serrano-Pertierra E et al. Characterization of plasma-derived extracellular vesicles isolated by different methods: A comparison study. Bioengineering, 2019.
22. Gristina V et al. Clinical Potential of Circulating Cell-Free DNA (cfDNA) for Longitudinally Monitoring Clinical Outcomes in the First-Line Setting of Non-Small-Cell Lung Cancer (NSCLC): A Real-World Prospective Study. Cancers (Basel)., 2022.
23. Théry C et al. Minimal information for studies of extracellular vesicles 2018 (MISEV2018): a position statement of the International Society for Extracellular Vesicles and update of the MISEV2014 guidelines. J Extracell Vesicles, 2018.
24. Taverna S et al. Role of exosomes released by chronic myelogenous leukemia cells in angiogenesis. Int J Cancer, 2012.
25. Taverna S et al. Amphiregulin contained in NSCLC-exosomes induces osteoclast differentiation through the activation of EGFR pathway. Sci Rep, 2017.
26. Noto R et al. The tempered polymerization of human neuroserpin. PLoS ONE, 2012.
27. Normak K et al. Multiparametric Orthogonal Characterization of Extracellular Vesicles by Liquid Chromatography Combined with In-Line Light Scattering and Fluorescence Detection. Anal Chem, 2023.
28. Adamo G et al. Nanoalgosomes: Introducing extracellular vesicles produced by microalgae. J Extracell Vesicles, 2021.
29. Romancino DP et al. Palmitoylation is a post-translational modification of Alix regulating the membrane organization of exosome-like small extracellular vesicles. Biochim Biophys Acta - Gen Subj, 2018.
30. Schmitz KS, Phillies GDJ. An Introduction to Dynamic Light Scattering by. Macromol Phys Today, 1991.
31. Liu SYM, Zheng MM, Pan Y, Liu SY, Li Y, Wu YL. Emerging evidence and treatment paradigm of non-small cell lung cancer. J Hematol Oncol. 2023.
32. Liu SY, Liao Y, Hosseinifard H, Imani S, Wen QL. Diagnostic Role of Extracellular Vesicles in Cancer: A Comprehensive Systematic Review and Meta-Analysis. Front Cell Dev Biology. 2021.
33. Amintas S et al. Next-Generation Cancer Biomarkers: Extracellular Vesicle DNA as a Circulating Surrogate of Tumor DNA. Front Cell Dev Biology. 2021.
34. Stam J, Bartel S, Bischoff R, Wolters JC. Isolation of extracellular vesicles with combined enrichment methods, Journal of Chromatography B: Analytical Technologies in the Biomedical and Life Sciences. 2021.

35. Mateescu B et al. Obstacles and opportunities in the functional analysis of extracellular vesicle RNA - An ISEV position paper. J Extracell Vesicles, 2017.
36. Vetsika EK et al. Small extracellular vesicles in pre-therapy plasma predict clinical outcome in non-small-cell lung cancer patients. Cancers (Basel)., 2021.
37. Maguire CM, Rösslein M, Wick P, Prina-Mello A. Characterisation of particles in solution–a perspective on light scattering and comparative technologies. Sci Technol Adv Mater. 2018.
38. Hood JL, Pan H, Lanza GM, Wickline SA. Paracrine induction of endothelium by tumor exosomes. Lab Investig, 2009.
39. Kogej K, Božič D, Kobal B, Herzog M, Černe K. Application of dynamic and static light scattering for size and shape characterization of small extracellular nanoparticles in plasma and ascites of ovarian cancer patients. Int J Mol Sci, 2021.
40. Lyu TS et al. The characterization of exosomes from fibrosarcoma cell and the useful usage of Dynamic Light Scattering (DLS) for their evaluation. PLoS ONE, 2021.
41. Sehgal K et al. Association of Performance Status with Survival in Patients with Advanced Non-Small Cell Lung Cancer Treated with Pembrolizumab Monotherapy. JAMA Netw Open, 2021.
42. Veerman RE et al. Molecular evaluation of five different isolation methods for extracellular vesicles reveals different clinical applicability and subcellular origin. J Extracell Vesicles, 2021.
43. Hinestrosa JP et al. Early-stage multi-cancer detection using an extracellular vesicle protein-based blood test. Commun Med, 2022.

Figures

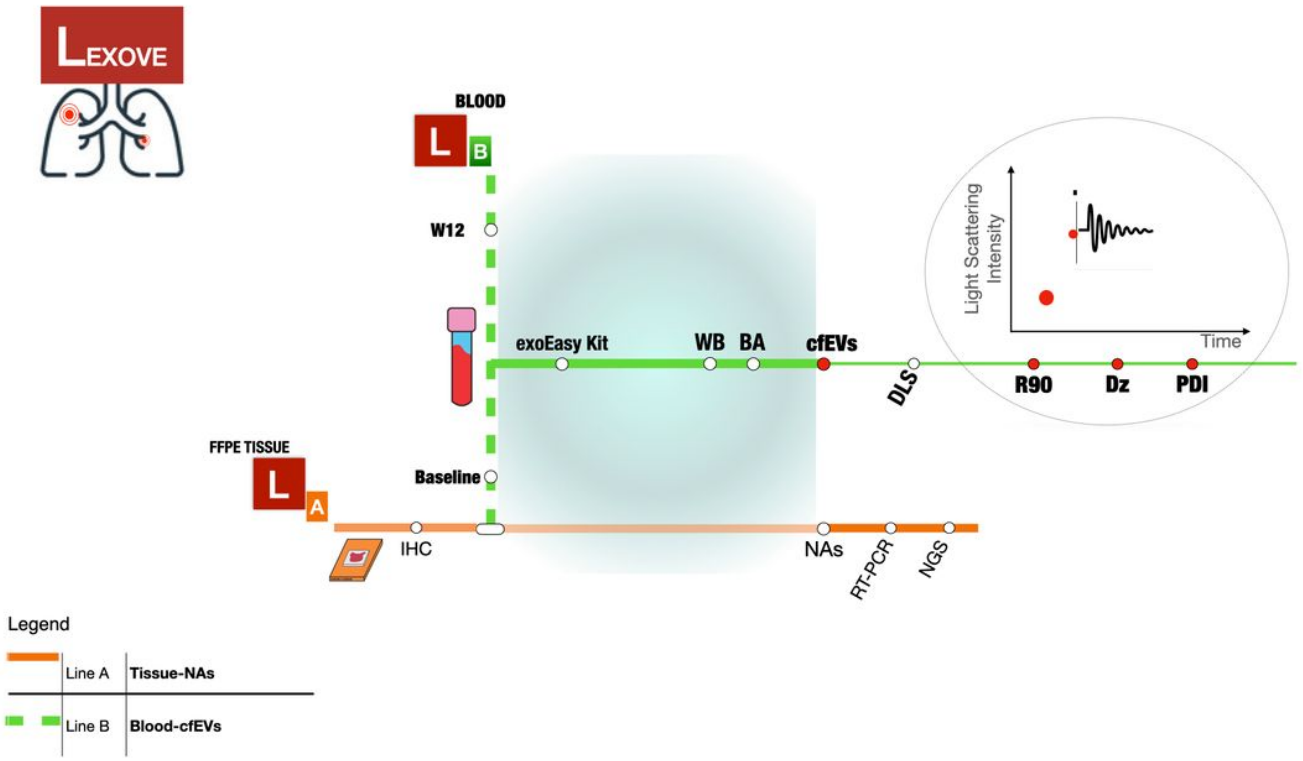

Figure 1

Graphical scheme design of the LEXOVE prospective study. Line A shows patients' accrual according to tissue predictive molecular pathology following clinical practice guidelines. Line B depicts complementary evaluation of plasma samples for extracellular vesicles (EVs) analyses at baseline and the first radiologic evaluation of disease within 12 ±1 weeks (W12): circulating EV isolation was carried out using serial centrifugation steps followed by a membrane affinity-based commercial method (exoEasy-kit); isolated EVs were characterized using either Western Blot (WB) to determine EV-based markers, Bradford assay (BA) for the quantification of circulating EV protein content (cell-free EV, cfEV) or Dynamic Light Scattering (DLS) to assess the amount and the size distribution of EVs (R90, Rayleigh ratio excess at angle 90°; Dz, z-averaged hydrodynamic diameter; PDI, polydispersity index). Abbreviations: IHC, immunohistochemistry; RT-PCR, real time-polymerase chain reaction; NA, nucleic acids; NGS, next-generation sequencing.

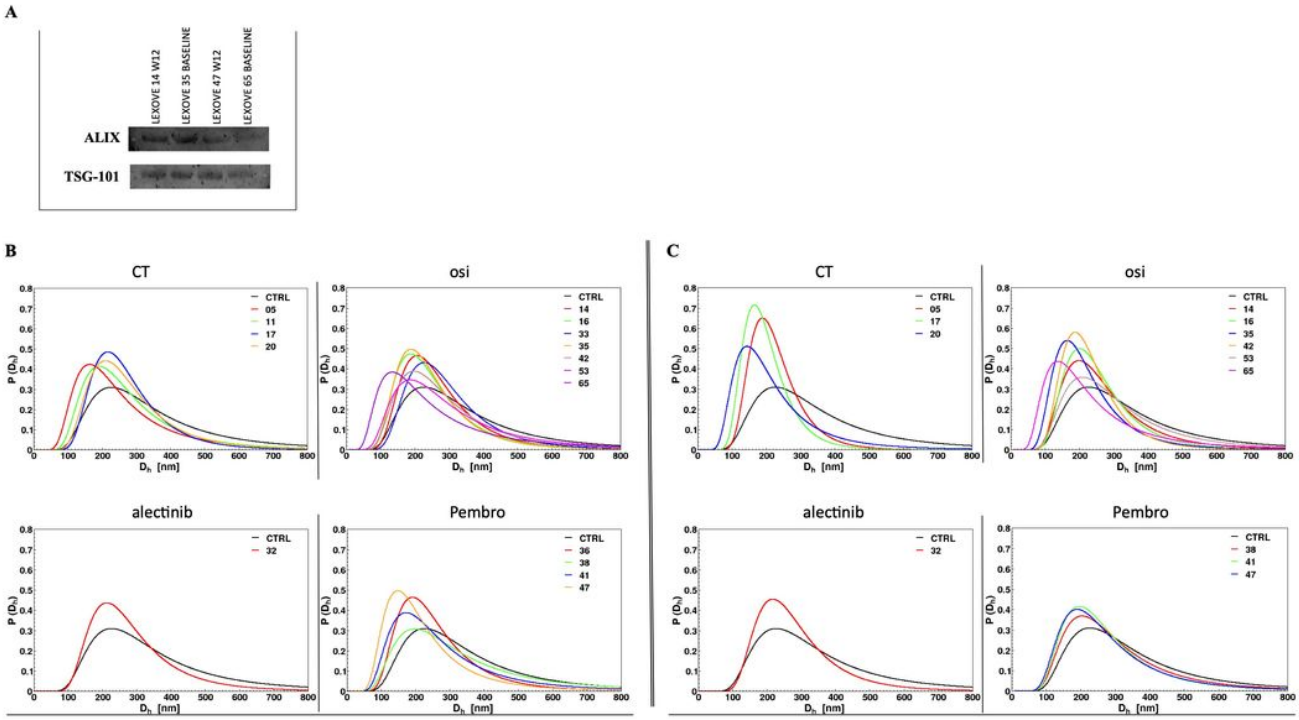

Figure 2

Extracellular vesicles (EVs) characterization: Western Blot showing positive EV staining for ALIX and TSG-101 (A); Dynamic Light Scattering analyses of EVs isolated from healthy controls and plasma of treatment-naïve patients with advanced NSCLC undergoing first-line systemic treatments at baseline (B) and after twelve weeks follow-up (C). Abbreviations: CTRL, healthy control; CT, chemotherapy; osi; osimertinib; pembro, pembrolizumab.

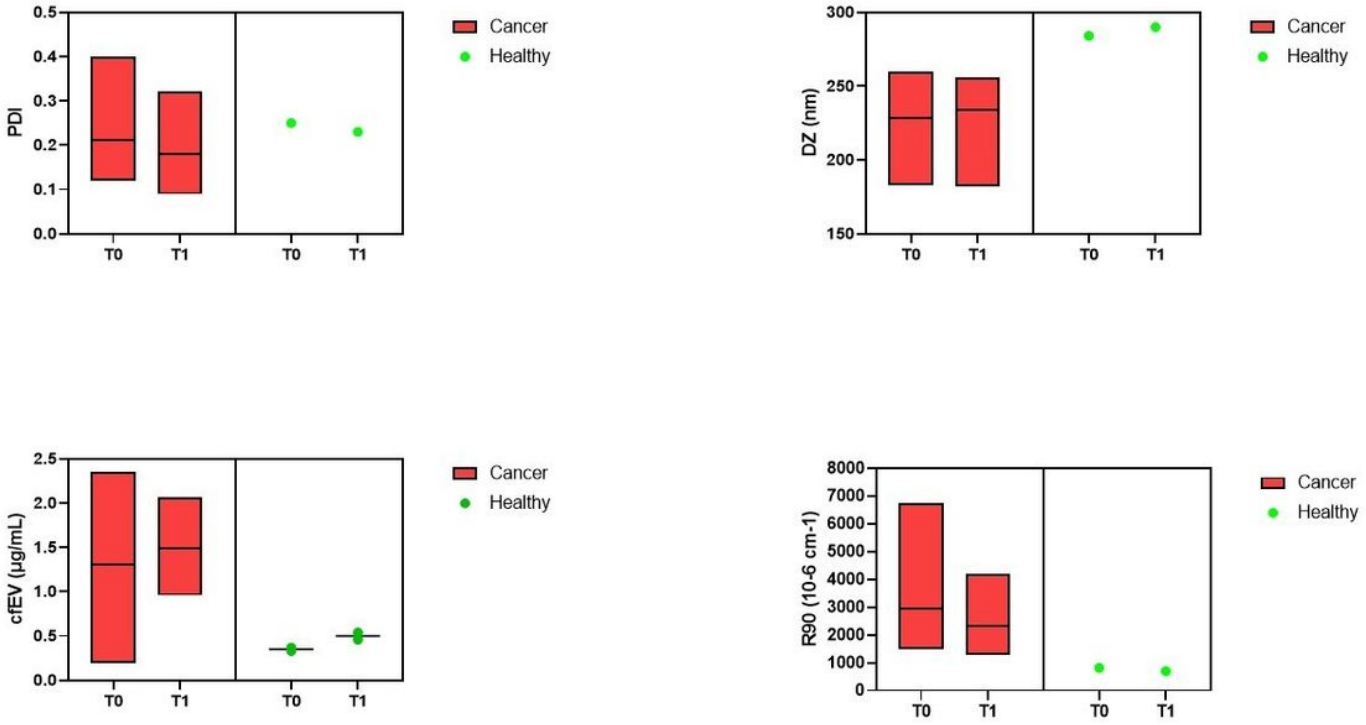

Figure 3

Box-and-whisker plots showing different median levels of plasma extracellular vesicles between cancer and healthy controls at baseline (T0) and after twelve weeks follow-up (T1) according to Bradford and Dynamic Light Scattering analyses. Abbreviations: cfEV, cell-free extracellular vesicle protein content; R90, excess Rayleigh ratio at 90°; Dz, z-averaged hydrodynamic diameter; PDI, polydispersity index

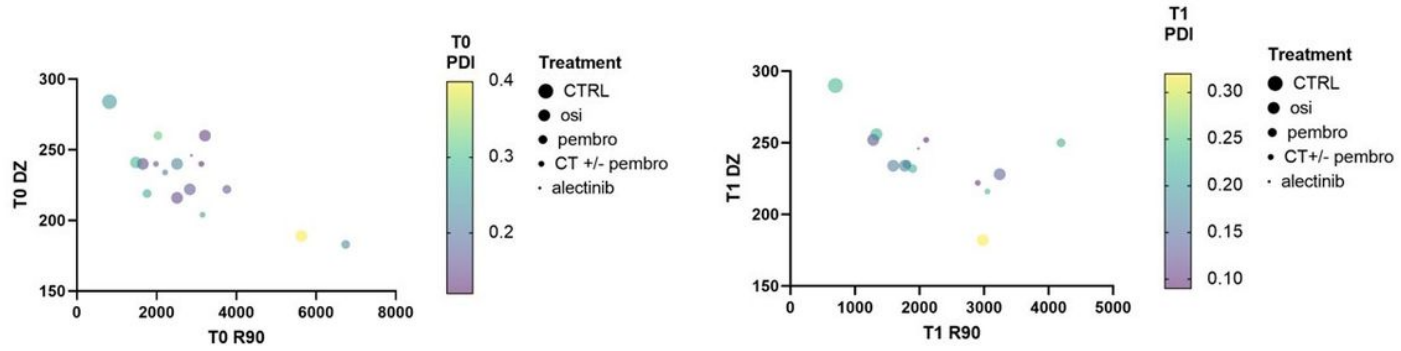

Figure 4

Dynamic Light Scattering showing amount (R90), size (Dz) and distribution (PDI) of extracellular vesicles between cancer and healthy controls at baseline (T0) and after twelve weeks follow-up (T1).
Abbreviations: R90, Rayleigh ratio; Dz, z-averaged hydrodynamic diameter; PDI, polydispersity index; CTRL, healthy control; CT, chemotherapy; osi; osimertinib; pembro, pembrolizumab

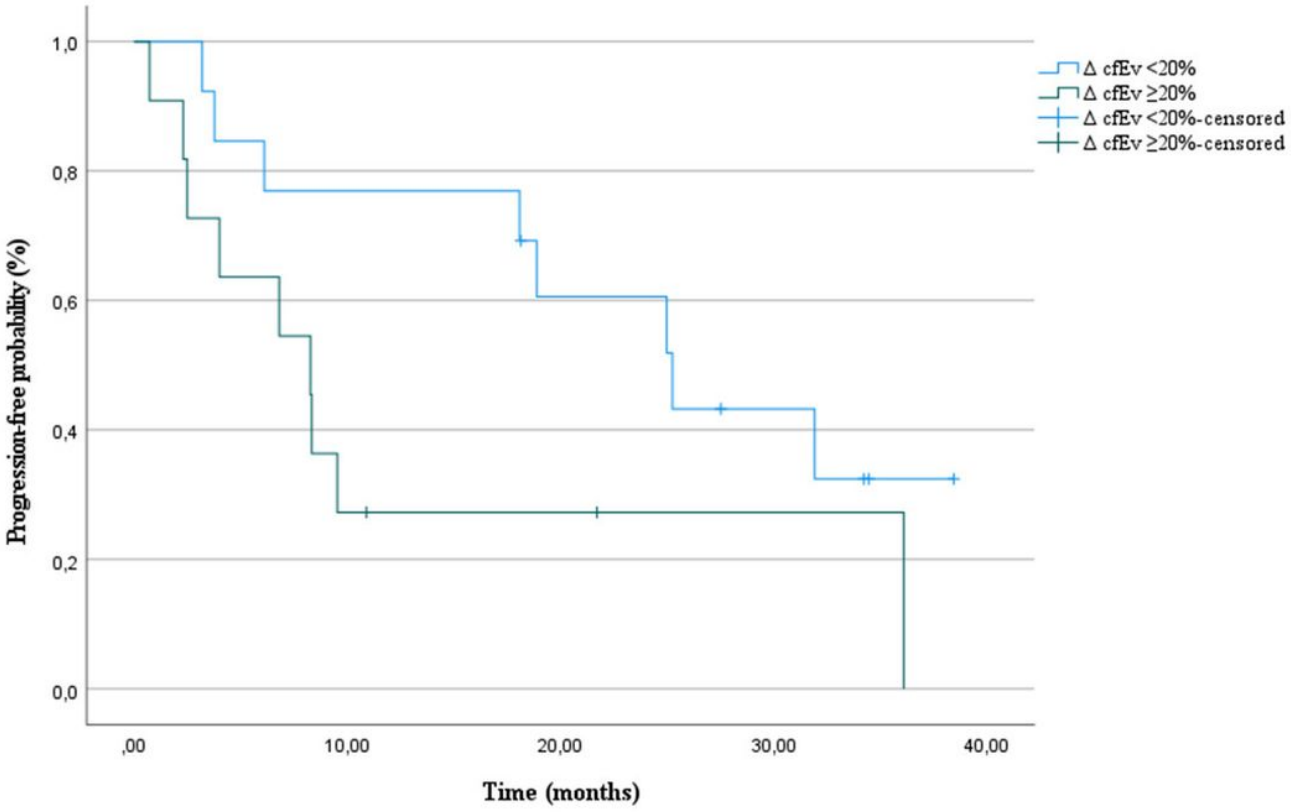

Figure 5

Kaplan–Meier analysis of progression-free survival according to Δ cfEV in the overall cohort population.

Abbreviations: Δ cfEV, cell-free extracellular vesicle protein levels from baseline to disease restaging.

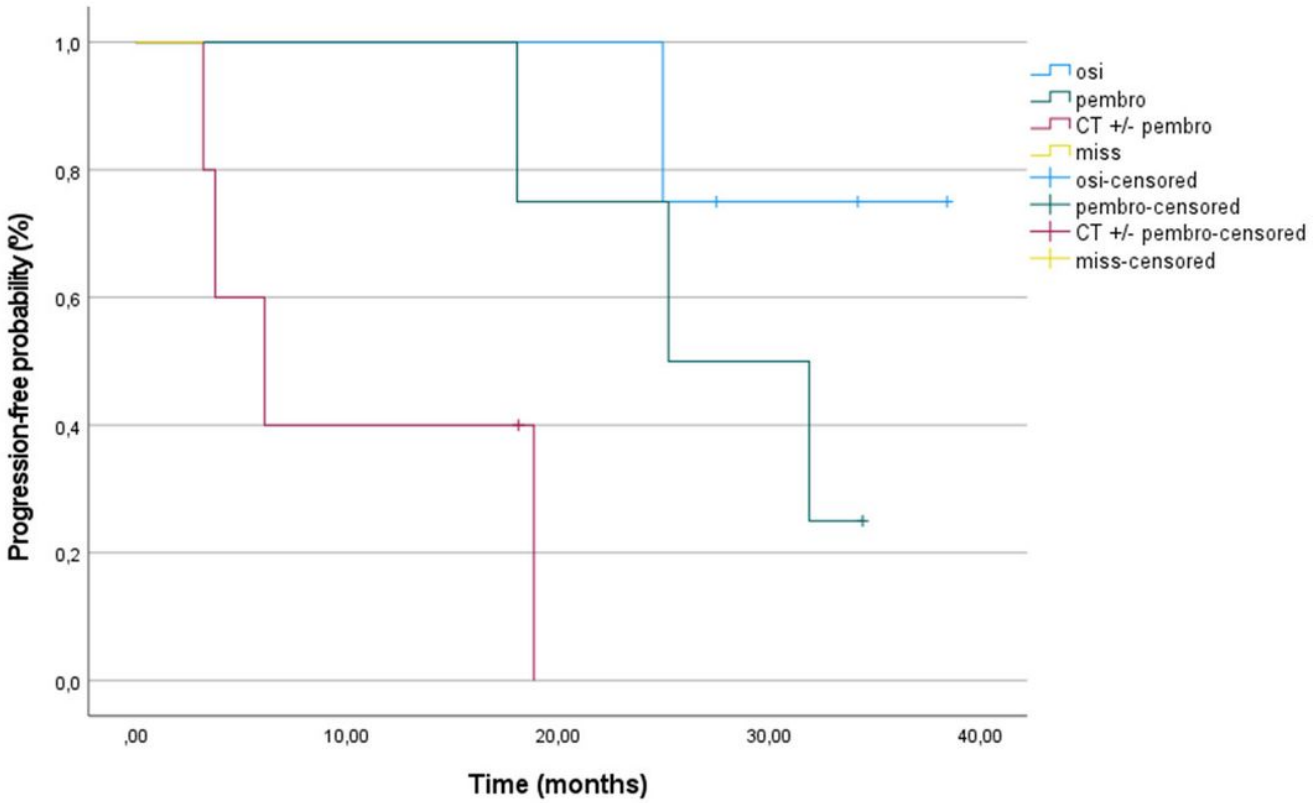

Figure 6

Kaplan–Meier analysis of PFS according to treatment subgroups in patients with Δ cfEV decrease.

Abbreviations: Δ cfEV, cell-free extracellular vesicle protein levels from baseline to disease restaging; osi, osimertinib; pembro, pembrolizumab; CT, platinum-based chemotherapy.

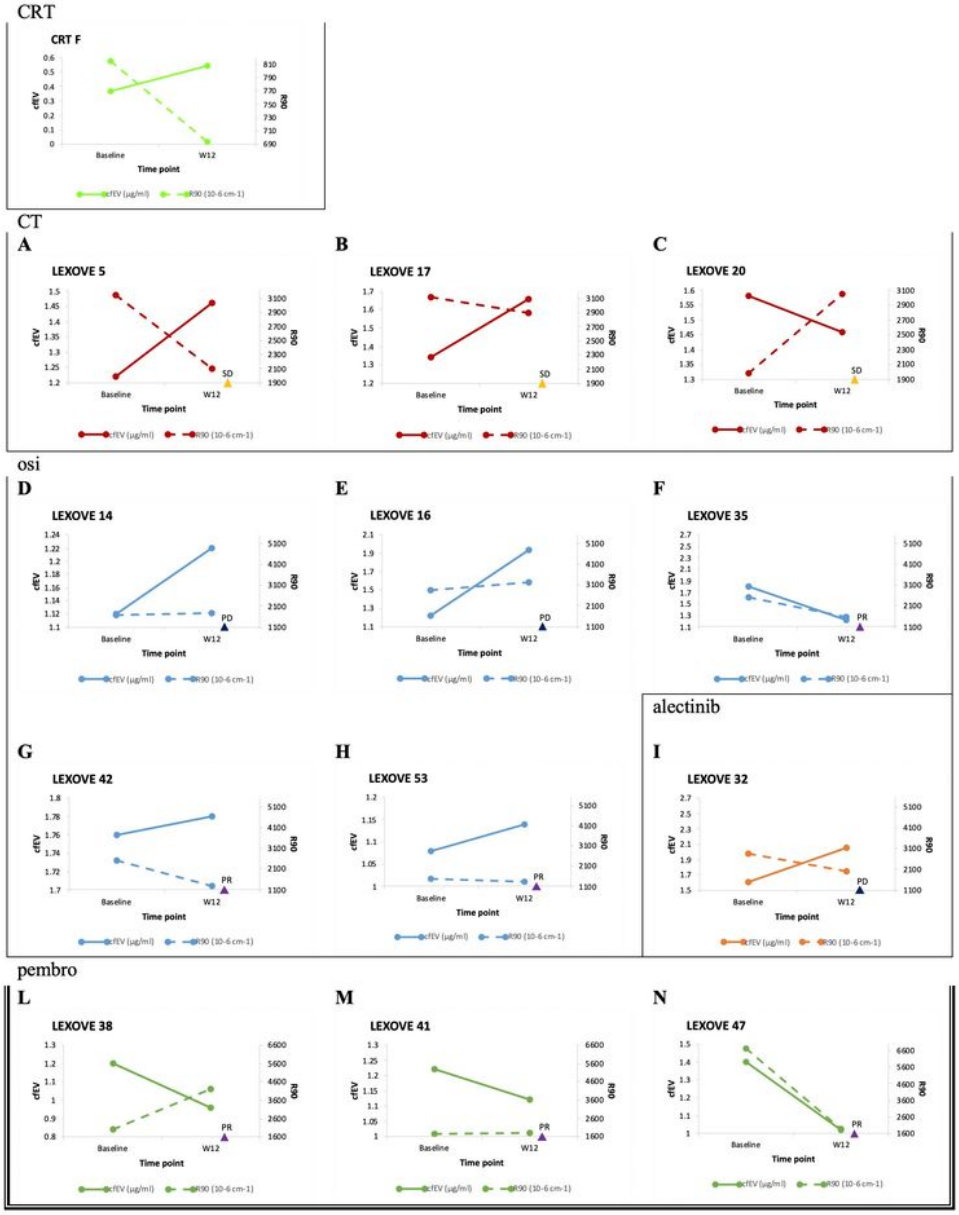

Figure 7

Graphical representation of the longitudinal monitoring according to the dynamics of amount (R90) and protein levels (cfEV) of extracellular vesicles (EVs) among different treatment subgroups. Abbreviations: CRT, healthy control; CT, chemotherapy; osi; osimertinib; pembro, pembrolizumab; W12, first disease restaging at twelve weeks; cfEV, cell-free extracellular vesicle protein levels; R90, the Rayleigh scattering values.

Supplementary Files

This is a list of supplementary files associated with this preprint. Click to download.

- AdditionalFile1.SupplementaryMethodsandResults.docx